Registration of Multimodal Remote Sensing Images Using Transfer Optimization

Xiaohu Yan, Yongjun Zhang, Dejun Zhang, Neng Hou, and Bin Zhang

***Abstract*—Multimodal image registration is critical yet challenging for remote sensing image processing. Due to the large nonlinear intensity differences between the multimodal images, conventional search algorithms tend to get trapped into local optima when optimizing the transformation parameters by maximizing mutual information (MI). To address this problem, inspired by transfer learning, we propose a novel search algorithm named transfer optimization (TO), which can be applied to any optimizer. In TO, an optimizer transfers its better individuals to the other optimizer in each iteration. Thus, TO can share information between two optimizers and take advantage of their search mechanisms, which is helpful to avoid the local optima. Then, the registration of the multimodal remote sensing images using TO is presented. We compare the proposed algorithm with several state-of-the-art algorithms on real and simulated image pairs. Experimental results demonstrate the superiority of our algorithm in terms of registration accuracy.**

***Index Terms*—Image registration, multimodal image, mutual information (MI), transfer optimization (TO), transformation parameters.**

I. Introduction

IMAGE registration is a fundamental task in many remote sensing applications, such as image fusion, image mosaic, and change detection [1]. The aim of image registration is to align the sensed image from different sensors, from different viewpoints, or at different times with a reference image. In recent years, considerable attention has been paid to the registration of multimodal remote sensing images to obtain the complementary and valuable information [2]. However, due to the nonlinear intensity differences and geometric deformations, the registration of multimodal images is still a challenging task [3].

Manuscript received September 24, 2019; revised November 21, 2019 and December 27, 2019; accepted December 28, 2019. Date of publication January 14, 2020; date of current version November 24, 2020. This work was supported in part by the National Key Research and Development Program of China under Grant 2018YFB0505003, in part by the National Natural Science Foundation of China under Grant 41871368 and Grant 41601352, and in part by the China Postdoctoral Science Foundation under Grant 2019M662709. *(Corresponding author: Yongjun Zhang.)*

Xiaohu Yan, Yongjun Zhang, and Bin Zhang are with the School of Remote Sensing and Information Engineering, Wuhan University, Wuhan 430079, China (e-mail: yanxiaohu@whu.edu.cn; zhangyj@whu.edu.cn; bin.zhang@whu.edu.cn).

Dejun Zhang is with the School of Geography and Information Engineering, China University of Geosciences, Wuhan 430074, China (e-mail: zhangdejun@cug.edu.cn).

Neng Hou is with the School of Computer Science, Yangtze University, Jingzhou 434023, China (e-mail: nhou@yangtzeu.edu.cn).

Color versions of one or more of the figures in this letter are available online at https://ieeexplore.ieee.org.

Digital Object Identifier 10.1109/LGRS.2019.2963477

Image registration methods are coarsely classified into feature-based and area-based methods [4]. The scale-invariant feature transform (SIFT) algorithm and its variants are the most famous algorithms to detect the features, because they are invariant to scale, rotation, and translation [5]. The speeded-up robust features (SURF) algorithm employs a Hessian matrix-based measure and improves the speed [6]. Affine-SIFT (ASIFT) achieves invariance to affine transformation by simulating all image views obtainable by varying two camera-axis-orientation parameters [7]. Synthetic aperture radar (SAR)-SIFT uses a new gradient definition, which yields an orientation and a magnitude that are robust to speckle noise [8]. Uniform robust SIFT (UR-SIFT) applies a selection strategy to extract high-quality SIFT features in the uniform distribution [9]. Adaptive binning SIFT (AB-SIFT) uses an adaptive histogram quantization strategy for both the location and gradient orientations [10]. The histogram of oriented self-similarity (HOSS) algorithm that is robust to illumination variations computes the histogram of self-similarity measures in multiple directions [11]. Ye *et al.* [12] presented a new feature descriptor named histogram of orientated phase congruency (HOPC) that can capture the geometric structural features of multimodal images. Chang *et al.* [13] proposed a novel registration algorithm for remote sensing images based on modified SIFT and feature slope grouping.

Due to the large nonlinear intensity differences between the multimodal images, it is difficult to detect highly repeatable common features by using feature-based methods in complex registration cases. Area-based methods that deal directly with the image intensity values can avoid the step of feature detection, and hence are effectively applied to multimodal image registration. Area-based methods can generally be classified into three categories: correlation-like methods, Fourier methods, and mutual information (MI) methods [14]. MI methods are the most popular in remote sensing image registration. An *et al.* [15] introduced a modified particle swarm optimization (PSO) method that reinitializes particle velocity to search for the maximum MI. Fan *et al.* [16] proposed an improved MI method that combines the spatial information through a feature-based selection mechanism. Liang *et al.* [17] proposed a novel similarity metric based on spatial and MI (SMI), and adopted ant colony optimization (ACO) to optimize SMI. Wu *et al.* [18] combined continuous ACO and local search operation to maximize MI.

Despite the impressive performance of MI methods, the similarity curve of MI has been shown to have many local optima in multimodal image registration [19]. Search algorithms tend to get trapped into the local optima when searching for the global optimum, which leads to poor registration performance. To address this problem, inspired by transfer learning [20], we propose a new approach for multimodal remote sensing image registration using transfer optimization (TO). TO is used to optimize the transformation parameters by maximizing MI. In TO, an optimizer transfers its better individuals to the other optimizer in each iteration, which is helpful to avoid local optima.

This letter is organized as follows. In Section II, multimodal image registration using TO is described. In Section III, experimental results and analysis are presented. Conclusions are summarized in Section IV.

II. Multimodal Image Registration Using TO

In this section, we present a novel approach for multimodal image registration that uses MI as the similarity measure and TO as the search algorithm.

A. Transformation Model

Current technologies can remove obvious geometric distortions and produce remote sensing images that have an offset of only dozen or so pixels [21]. Moreover, remote sensing images can be resampled to the same ground sample distance (GSD) to eliminate the scale differences [12]. Thus, we adopt the rigid transformation model in the registration of multimodal remote sensing images. The translations of the x-axis and the y-axis are denoted as t_x and t_y, respectively. The rotation is denoted as θ. Then, the rigid transformation model can be formulated as

$$\begin{bmatrix} x' \\ y' \end{bmatrix} = \begin{bmatrix} \cos\theta & -\sin\theta \\ \sin\theta & \cos\theta \end{bmatrix} \begin{bmatrix} x \\ y \end{bmatrix} + \begin{bmatrix} t_x \\ t_y \end{bmatrix}. \tag{1}$$

B. MI

According to the information theoretic notion of entropy, MI of images A and B can be computed by

$$I(A, B) = H(A) + H(B) - H(A, B) \tag{2}$$

where $H(A)$ and $H(B)$ are the marginal entropies of images A and B, respectively, and $H(A, B)$ is their joint entropy. The entropies and joint entropy can be computed by

$$H(A) = -\sum_{a} P_A(a)\log_2 P_A(a) \tag{3}$$

$$H(B) = -\sum_{b} P_B(b)\log_2 P_B(b) \tag{4}$$

$$H(A, B) = -\sum_{a,b} P_{AB}(a, b)\log_2 P_{AB}(a, b) \tag{5}$$

where $P_A(a)$ and $P_B(b)$ are the marginal probability distributions of images A and B, respectively, and $P_{AB}(a, b)$ is their joint probability distribution [22].

C. TO

To solve the complex optimization problems, many optimizers with different search mechanisms have been proposed over the last few decades. In an iteration, individuals from an optimizer may have unexploited and unexplored positions that can help the other optimizer find better solutions. Inspired by transfer learning, we propose TO that transfers individuals between two optimizers. Specifically, in each iteration, an optimizer transfers its better individuals to the other optimizer. The pseudocode of TO is presented in Algorithm 1.

Algorithm 1 Search Algorithm TO

```
Input: M, the maximum number of iterations;
       N, the population size;
       T_c, the threshold number of iterations;
       opt_1, the first optimizer;
       opt_2, the second optimizer.
Output: gx, the global best position.
Randomly generate N individuals to initialize the
population of opt_1 named pop_1;
Randomly generate N individuals to initialize the
population of opt_2 named pop_2;
for t = 1 : M do
  | Compute the fitness of each individual in pop_1 and
  | pop_2;
  | Update pop_1 according to the search mechanism of
  | opt_1;
  | Update pop_2 according to the search mechanism of
  | opt_2;
  | for i = 1 : N do
  |   | if the fitness of pop_1(i) is better than that of
  |   | pop_2(i) then
  |   |   | pop_2(i)=pop_1(i);
  |   | end
  |   | else
  |   |   | pop_1(i)=pop_2(i);
  |   | end
  | end
  | Update the global best position and its fitness;
  | if the global best fitness has not been improved in T_c
  | iterations then
  |   | break;
  | end
end
```

In TO, two optimizers run independently according to their search mechanisms. Then, the convergence of TO can be ensured by the search mechanisms of two optimizers that are not disturbed by TO. After the population is updated, two optimizers transfer their better individuals to each other. Thus, TO can share information or knowledge between the two optimizers and take advantage of their search mechanisms, which is helpful to avoid local optima. Due to its convergence, TO is stopped when the global best fitness has not been improved in T_c iterations, which can reduce the runtime.

It is worthwhile to mention that TO can be applied to any optimizer. In this letter, we select PSO and the whale optimization algorithm (WOA). PSO is inspired by the intelligent behavior of birds or fish, and WOA simulates the hunting behavior of humpback whales. Thus, the search mechanisms

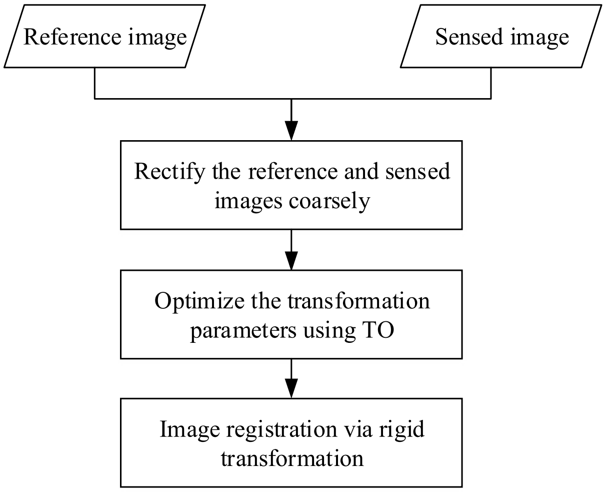

Fig. 1. Flowchart of multimodal image registration using TO.

of PSO and WOA are distinct and complementary, which can increase the population diversity and enhance the global search ability.

D. Multimodal Image Registration Using TO

TO is used to optimize the transformation parameters of multimodal images. In each iteration, the fitness is the value of MI, and the position of each individual consists of the transformation parameters t_x, t_y, and θ. The registration of multimodal remote sensing images using TO is presented in Fig. 1.

As shown in Fig. 1, we first rectify the reference and sensed images coarsely by using the direct georeferencing techniques. Hence, the obvious geometric distortions of multimodal remote sensing images are removed. Second, TO optimizes the transformation parameters by maximizing MI. We compute the MI of each individual in all iterations. Two optimizers transfer their individuals according to the value of MI. The global best position is the optimal transformation parameters obtained by TO. Finally, we register the sensed image by rigid transformation according to (1).

III. Experiments

To verify the effectiveness of the proposed algorithm, we compare TO with several state-of-the-art algorithms such as SIFT [5] and HOPC [12]. To investigate its performance further, TO is compared with PSO, WOA, and Powell [23]. In the feature-based methods, we use the fast sample consensus (FSC) algorithm [24] to estimate the transformation parameters.

A. Experimental Setup

In TO, the population size is 30. To compare fairly, the population size is set to 60 in PSO and WOA, because there are two optimizers in TO. In PSO, the learning factors are 2, and the inertial weight is decreased linearly from 0.9 to 0.2 over iterations. In PSO, WOA, Powell, and TO, the maximum number of iterations is 500, and T_c is 20. The parameters of SIFT, HOPC, Powell, WOA, and FSC are set according to their original literature.

The search ranges of t_x, t_y, and θ are set to [−20, −20, −20; 20, 20, 20]. The algorithms are written in MATLAB R2018a. All experiments are executed on an Intel Core i7-8700 at 3.2 GHz CPU with 8-GB memory.

B. Evaluation Criterion

The root-mean-square error (RMSE) and mean absolution error (MAE) of the check points are used to evaluate registration accuracy quantitatively. L check points $\{(x_i, y_i), (x_i', y_i')\}$ are selected from the reference and sensed images. Let (x_i'', y_i'') denote the transformed coordinates of (x_i', y_i'). Then, RMSE and MAE are computed by

$$\text{RMSE} = \sqrt{\frac{1}{L}\sum_{i=1}^{L}\left(\left(x_i - x_i''\right)^2 + \left(y_i - y_i''\right)^2\right)} \quad (6)$$

$$\text{MAE} = \frac{1}{L}\sum_{i=1}^{L}\sqrt{\left(\left(x_i - x_i''\right)^2 + \left(y_i - y_i''\right)^2\right)}. \quad (7)$$

In general, the check points are determined manually. Specifically, for each image pair, we select 40–60 evenly distributed check points with a subpixel accuracy between the reference and sensed images. The runtime is employed to evaluate computational efficiency. Moreover, we use the value of MI to analyze the search ability of TO.

C. Description of Data Sets

We test the proposed algorithm on six pairs of real multimodal images, which are shown in Fig. 2. In Fig. 2, the reference images are presented in the first row, and the sensed images are presented in the second row.

As shown in Fig. 2, image pair 1 is from Daedalus visible and infrared data on April 2000. The two images are 512 × 512 with a spatial resolution of 0.5 m [12]. Image pair 2 is from Landsat 5 Thematic Mapper (TM) infrared and visible data with a spatial resolution of 30 m. The two images with 588 × 606 are captured over Jiangsu Province, China. Image pair 3 is airborne light detection and ranging (LiDAR) and visible images. The two images are 480 × 550 with a spatial resolution of 0.8 m. Image pair 4 is captured over Tibet Province, China. The two images with 531 × 455 are downloaded from Google Maps. Image pair 5 is from Google Earth on November 2009 and TerraSAR-X on December 2008 [3]. The two images are 618 × 628 with a spatial resolution of 3 m. Image pair 6 is from Landsat 5 TM and Sentinel-1A. The two images with 688 × 500 are captured over Kyushu, Japan.

To increase the difficulty of image registration, we test the proposed algorithm on six pairs of synthetic multimodal images. The synthetic image pairs are simulated by real image pairs. Specifically, the sensed images of image pairs 1–6 suffer 8° rotations to produce the sensed images of image pairs 7–12. The sensed images of synthetic image pairs are shown in Fig. 3.

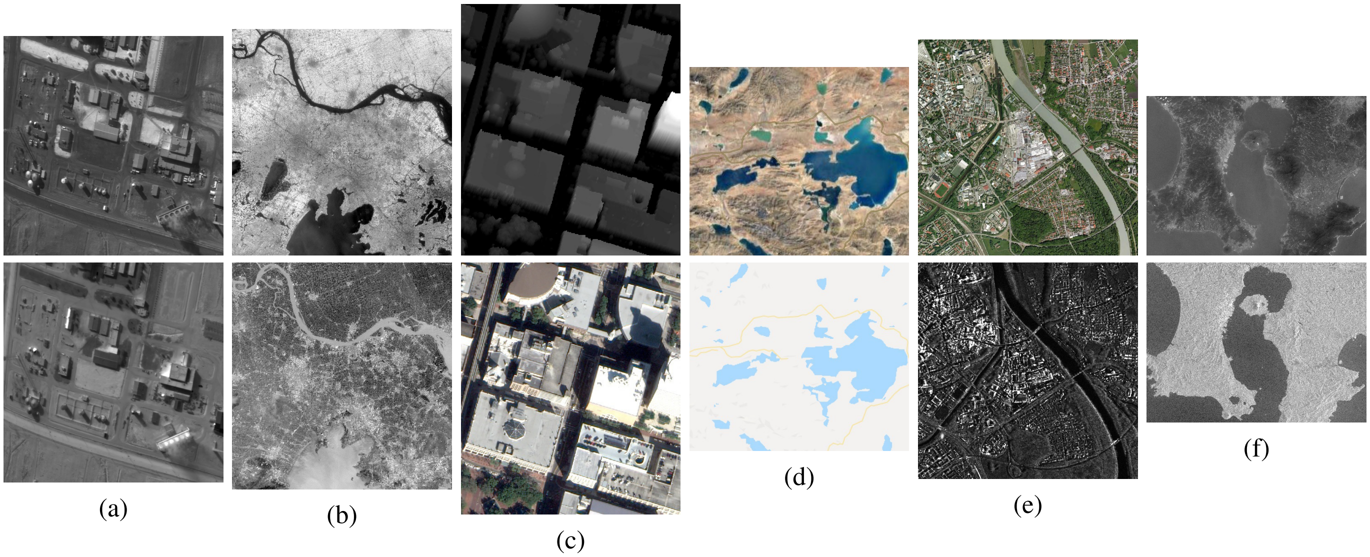

Fig. 2. Multimodal image pairs. (a) Image pair 1. (b) Image pair 2. (c) Image pair 3. (d) Image pair 4. (e) Image pair 5. (f) Image pair 6.

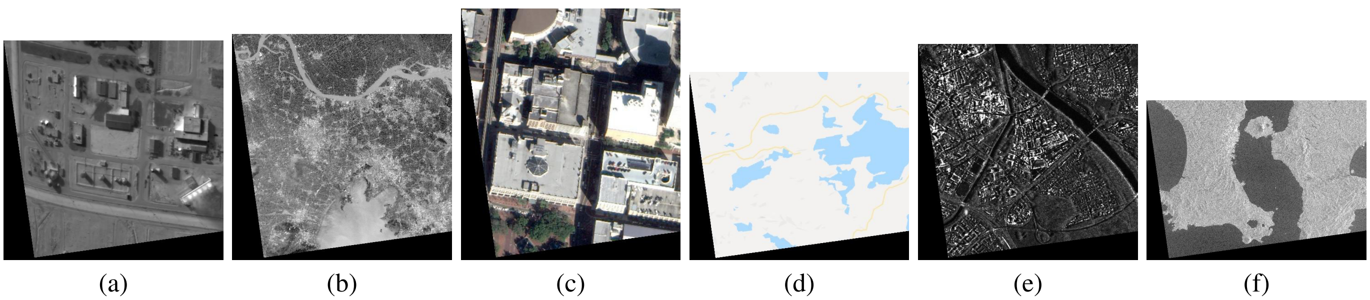

Fig. 3. Sensed images of synthetic image pairs. (a) Image pair 7. (b) Image pair 8. (c) Image pair 9. (d) Image pair 10. (e) Image pair 11. (f) Image pair 12.

TABLE I

RMSE, MAE, AND RUNTIME COMPARISONS OF SIFT, HOPC, PSO, WOA, POWELL, AND TO

Method	Criterion	Image pair											
		1	2	3	4	5	6	7	8	9	10	11	12
SIFT	RMSE	0.4644	387.5597	337.3790	1.8492	313.0049	275.7280	0.9301	691.1652	265.9522	1.9511	653.4436	283.9468
	MAE	0.4018	352.6355	315.1028	1.4750	275.7793	231.9987	0.8892	640.3585	239.5720	1.6557	616.9826	237.2223
	Runtime	1.6333	3.3325	1.8005	1.6769	8.2658	1.6169	1.4909	3.6782	1.9182	1.6554	8.9115	1.7631
HOPC	RMSE	0.3990	0.9573	1.2245	1.6335	1.6135	1.4292	0.5389	1.8107	1.1692	1.6950	1.1242	1.9628
	MAE	0.3732	0.8625	1.1739	1.3770	1.5024	1.1688	0.4962	1.6274	1.0240	1.4586	1.0102	1.7136
	Runtime	23.4184	20.9670	20.4489	20.4807	20.8868	20.4061	20.6644	17.9665	16.9437	18.1147	17.9162	16.9648
PSO	RMSE	0.7873	1.1808	1.3687	1.9767	1.2063	1.8361	0.9130	1.3328	1.5445	2.4139	1.5930	1.4168
	MAE	0.7287	1.0210	1.3277	1.5722	1.0988	1.6460	0.8894	1.2521	1.2491	2.0857	1.2191	1.2254
	Runtime	15.6062	17.6461	29.4498	13.1843	20.8444	12.3201	21.9341	19.9450	24.1641	16.6117	18.9286	14.1535
WOA	RMSE	0.3108	0.8984	1.1154	1.6698	1.1199	2.3953	1.5094	1.4628	1.7196	2.2110	1.7149	1.6533
	MAE	0.2295	0.7824	**0.5045**	1.2448	**0.7591**	2.2514	1.4151	1.3145	1.6070	1.9335	1.3582	1.4975
	Runtime	43.2237	45.2954	55.2742	53.6935	44.4057	21.7685	78.7438	90.1503	25.5416	33.1719	26.0101	26.5829
Powell	RMSE	0.6302	0.9031	5.7758	2.1191	1.4724	7.6714	45.6987	62.1947	55.0934	2.2670	70.5015	75.8493
	MAE	0.5833	0.7818	5.6996	1.7414	1.3809	7.6306	42.9267	52.4136	50.7141	1.9380	69.4105	71.3183
	Runtime	7.0431	9.7951	7.0374	11.9218	14.0273	13.2785	7.2886	7.7487	7.0871	12.2063	21.8111	14.9523
TO	RMSE	**0.2927**	**0.8781**	**1.0628**	**1.5791**	**0.9647**	**1.3264**	**0.5094**	**0.9370**	**1.0790**	**1.5900**	**0.9274**	**1.3621**
	MAE	**0.2243**	**0.7752**	0.5085	**0.9420**	0.8972	**1.1127**	**0.4793**	**0.8425**	**0.7174**	**1.1461**	**0.5168**	**1.1583**
	Runtime	62.2701	96.2492	72.9065	27.2769	20.5045	17.9939	25.6896	98.7976	37.8210	76.1598	27.6540	25.7742

D. Performance Evaluation

To analyze the performance of TO, we compare the algorithm with SIFT, HOPC, PSO, WOA, and Powell. RMSE, MAE, and runtime comparisons are presented in Table I. In Table I, the best result is marked in bold.

As can be seen in Table I, RMSE and MAE of TO are smaller than those of the other algorithms on most image pairs. Moreover, TO achieves satisfactory and accurate registration results in all types of multimodal image pairs, which confirms the effectiveness and robustness of TO. RMSE and MAE of

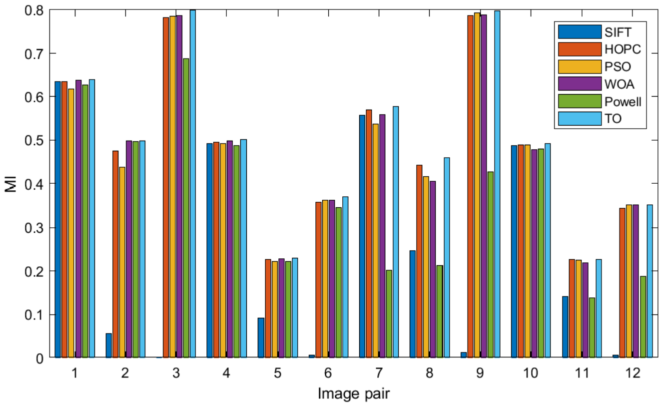

Fig. 4. MI comparison.

TO are significantly smaller than those of PSO and WOA, which demonstrates that the proposed transfer strategy is helpful to enhance registration accuracy. RMSE and MAE of SIFT are very large on most image pairs, because SIFT cannot detect highly repeatable shared features between the multimodal images.

It can be seen from Table I that the runtime of TO is larger than that of PSO and WOA on some image pairs, such as image pairs 1, 2, and 8. This result could be attributed to the fact that these algorithms are stopped when the global best fitness has not been improved in 20 iterations. To evaluate the search ability of TO, the value of MI is compared in Fig. 4.

As shown in Fig. 4, MI of TO is larger than that of the other algorithms on all image pairs. MI of SIFT is very small on most image pairs, which leads to failed registration. Compared with PSO and WOA, the improvement of MI in TO is obvious, which confirms that the proposed transfer strategy can increase the population diversity and enhance the global search ability. Therefore, TO is efficient for the registration of multimodal remote sensing images.

IV. Conclusion

In this letter, we propose a new approach for multimodal remote sensing image registration using TO. To avoid local optima, TO is used to optimize the transformation parameters. In each iteration, an optimizer transfers its better individuals to the other optimizer, which can help enhance the global search ability of TO. It is worth mentioning that TO can be applied to any optimizer. Experimental results on various multimodal remote sensing images demonstrate that the proposed algorithm outperforms the state-of-the-art algorithms in terms of registration accuracy. In the future, we will accelerate the calculation process of TO by using the graphics processing unit (GPU).

References

[1] J. Ma, J. Jiang, H. Zhou, J. Zhao, and X. Guo, "Guided locality preserving feature matching for remote sensing image registration," *IEEE Trans. Geosci. Remote Sens.*, vol. 56, no. 8, pp. 4435–4447, Aug. 2018.

[2] J. M. Murphy, J. Le Moigne, and D. J. Harding, "Automatic image registration of multimodal remotely sensed data with global shearlet features," *IEEE Trans. Geosci. Remote Sens.*, vol. 54, no. 3, pp. 1685–1704, Mar. 2016.

[3] J. Zhang, W. Ma, Y. Wu, and L. Jiao, "Multimodal remote sensing image registration based on image transfer and local features," *IEEE Geosci. Remote Sens. Lett.*, vol. 16, no. 8, pp. 1210–1214, Aug. 2019.

[4] F. Ye, Y. Su, H. Xiao, X. Zhao, and W. Min, "Remote sensing image registration using convolutional neural network features," *IEEE Geosci. Remote Sens. Lett.*, vol. 15, no. 2, pp. 232–236, Feb. 2018.

[5] D. G. Lowe, "Distinctive image features from scale-invariant keypoints," *Int. J. Comput. Vis.*, vol. 60, no. 2, pp. 91–110, Nov. 2004.

[6] H. Bay, T. Tuytelaars, and L. Van Gool, "Surf: Speeded up robust features," in *Computer Vision—ECCV*. Berlin, Germany: Springer, 2006, pp. 404–417.

[7] J.-M. Morel and G. Yu, "ASIFT: A new framework for fully affine invariant image comparison," *SIAM J. Imag. Sci.*, vol. 2, no. 2, pp. 438–469, Jan. 2009.

[8] F. Dellinger, J. Delon, Y. Gousseau, J. Michel, and F. Tupin, "SAR–SIFT: A SIFT-like algorithm for SAR images," *IEEE Trans. Geosci. Remote Sens.*, vol. 53, no. 1, pp. 453–466, Jan. 2015.

[9] A. Sedaghat, M. Mokhtarzade, and H. Ebadi, "Uniform robust scale-invariant feature matching for optical remote sensing images," *IEEE Trans. Geosci. Remote Sens.*, vol. 49, no. 11, pp. 4516–4527, Nov. 2011.

[10] A. Sedaghat and H. Ebadi, "Remote sensing image matching based on adaptive binning SIFT descriptor," *IEEE Trans. Geosci. Remote Sens.*, vol. 53, no. 10, pp. 5283–5293, Oct. 2015.

[11] A. Sedaghat and N. Mohammadi, "Illumination-robust remote sensing image matching based on oriented self-similarity," *ISPRS J. Photogram. Remote Sens.*, vol. 153, pp. 21–35, Jul. 2019.

[12] Y. Ye, J. Shan, L. Bruzzone, and L. Shen, "Robust registration of multimodal remote sensing images based on structural similarity," *IEEE Trans. Geosci. Remote Sens.*, vol. 55, no. 5, pp. 2941–2958, May 2017.

[13] H.-H. Chang, G.-L. Wu, and M.-H. Chiang, "Remote sensing image registration based on modified SIFT and feature slope grouping," *IEEE Geosci. Remote Sens. Lett.*, vol. 16, no. 9, pp. 1363–1367, Sep. 2019.

[14] B. Zitová and J. Flusser, "Image registration methods: A survey," *Image Vis. Comput.*, vol. 21, no. 11, pp. 977–1000, Oct. 2003.

[15] R. An *et al.*, "A modified PSO algorithm for remote sensing image template matching," *Photogramm. Eng. Remote Sens.*, vol. 76, no. 4, pp. 379–389, Apr. 2010.

[16] X. Fan, H. Rhody, and E. Saber, "A spatial-feature-enhanced MMI algorithm for multimodal airborne image registration," *IEEE Trans. Geosci. Remote Sens.*, vol. 48, no. 6, pp. 2580–2589, Jun. 2010.

[17] J. Liang, X. Liu, K. Huang, X. Li, D. Wang, and X. Wang, "Automatic registration of multisensor images using an integrated spatial and mutual information (SMI) metric," *IEEE Trans. Geosci. Remote Sens.*, vol. 52, no. 1, pp. 603–615, Jan. 2014.

[18] Y. Wu, W. Ma, Q. Miao, and S. Wang, "Multimodal continuous ant colony optimization for multisensor remote sensing image registration with local search," *Swarm Evol. Comput.*, vol. 47, pp. 89–95, Jun. 2019.

[19] F. Wang and B. C. Vemuri, "Non-rigid multi-modal image registration using cross-cumulative residual entropy," *Int. J. Comput. Vis.*, vol. 74, no. 2, pp. 201–215, May 2007.

[20] S. J. Pan and Q. Yang, "A survey on transfer learning," *IEEE Trans. Knowl. Data Eng.*, vol. 22, no. 10, pp. 1345–1359, Oct. 2010.

[21] H. Gonçalves, J. A. Gonçalves, L. Corte-Real, and A. C. Teodoro, "CHAIR: Automatic image registration based on correlation and Hough transform," *Int. J. Remote Sens.*, vol. 33, no. 24, pp. 7936–7968, Dec. 2012.

[22] X. Yan, F. He, Y. Zhang, and X. Xie, "An optimizer ensemble algorithm and its application to image registration," *Integr. Comput.-Aided Eng.*, vol. 26, no. 4, pp. 311–327, Sep. 2019.

[23] J. Du, S. Tang, T. Jiang, and Z. Lu, "Intensity-based robust similarity for multimodal image registration," *Int. J. Comput. Math.*, vol. 83, no. 1, pp. 49–57, Jan. 2006.

[24] Y. Wu, W. Ma, M. Gong, L. Su, and L. Jiao, "A novel point-matching algorithm based on fast sample consensus for image registration," *IEEE Geosci. Remote Sens. Lett.*, vol. 12, no. 1, pp. 43–47, Jan. 2015.